Force Nanoscopy of Hydrophobic Interactions in the Fungal Pathogen *Candida glabrata*

Sofiane El-Kirat-Chatel,[†,⊥] Audrey Beaussart,[†,⊥] Sylvie Derclaye,[†] David Alsteens,[†] Soňa Kucharíková,[‡,§] Patrick Van Dijck,[*,‡,§] and Yves F. Dufrêne[*,†]

[†]Institute of Life Sciences, Université Catholique de Louvain, Croix du Sud, 1, bte L7.04.01, B-1348 Louvain-la-Neuve, Belgium, [‡]Department of Molecular Microbiology, VIB, KU Leuven, B-3001 Leuven, Belgium, and [§]Laboratory of Molecular Cell Biology, Institute of Botany and Microbiology, K.U. Leuven, B-3001 Leuven, Belgium. [⊥]These authors (S.E.-K.-C. and A.B.) contributed equally to this work.

ABSTRACT

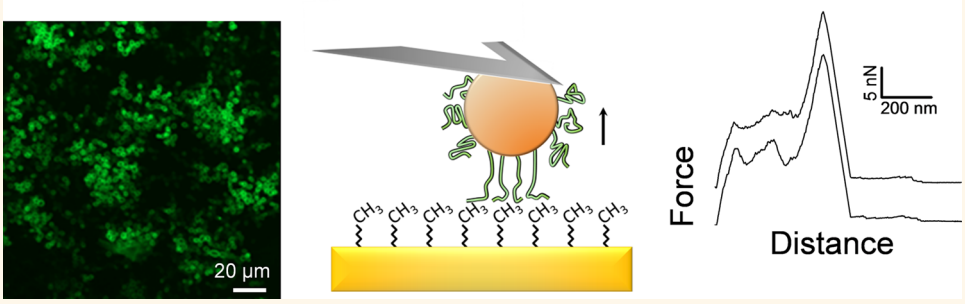

Candida glabrata is an opportunistic human fungal pathogen which binds to surfaces mainly through the Epa family of cell adhesion proteins. While some Epa proteins mediate specific lectin-like interactions with human epithelial cells, others promote adhesion and biofilm formation on plastic surfaces *via* nonspecific interactions that are not yet elucidated. We report the measurement of hydrophobic forces engaged in Epa6-mediated cell adhesion by means of atomic force microscopy (AFM). Using single-cell force spectroscopy, we found that *C. glabrata* wild-type (WT) cells attach to hydrophobic surfaces *via* strongly adhesive macromolecular bonds, while mutant cells impaired in Epa6 expression are weakly adhesive. Nanoscale mapping of yeast cells using AFM tips functionalized with hydrophobic groups shows that Epa6 is massively exposed on WT cells and conveys strong hydrophobic properties to the cell surface. Our results demonstrate that Epa6 mediates strong hydrophobic interactions, thereby providing a molecular basis for the ability of this adhesin to drive biofilm formation on abiotic surfaces.

KEYWORDS: atomic force microscopy · single-cell force spectroscopy · chemical force microscopy · hydrophobic forces · adhesion · fungal pathogens · *Candida glabrata* · Epa6

Many fungal infections involve the formation of biofilms on implanted devices such as prosthetics and catheters.[1−4] Although the mechanisms underlying the formation of *Candida albicans* biofilms have been well-established, much less is known about biofilms formed by the non-*C. albicans* species. In *Candida glabrata*, adhesion and biofilm development are mediated by cell adhesion proteins, primarily the Epa family of adhesins.[5,6] With the use of microscopic adhesion assays and electron microscopy, *C. glabrata* was shown to adhere avidly to human epithelial cells in culture.[7] By means of genetic tools, Epa1 was found to mediate specific lectin-like interactions between the yeast cells and host-cell carbohydrates.[7] In addition, *C. glabrata* is also capable to form biofilms on various plastic surfaces, implying that nonspecific interactions are also involved in fungal adhesion.[8,9] Use of a genetic screening strategy enabled to identify Epa6 as the principal adhesin involved in biofilm formation.[8,9] To date, the molecular interactions involved in Epa6-mediated adhesion are not established. Clearly, enhancing our understanding of Epa6-dependent interactions may contribute to the development of novel strategies for combating biofilm infections.

Like the widely investigated Flo (*Saccharomyces cerevisiae*) and Als (*C. albicans*)

* Address correspondence to Yves.Dufrene@uclouvain.be, Patrick.VanDijck@mmbio.vib-kuleuven.be.

Received for review November 7, 2014 and accepted January 19, 2015.

Published online January 26, 2015
10.1021/nn506370f

yeast adhesins, Epa proteins are made of multiple domains with discrete functions, *i.e.*, an N-terminal, well-folded ligand-binding domain, a Thr-rich midpiece composed of tandem repeats, a Ser- and Thr-rich tail that is probably in an extended conformation with little regular structure, and a C-terminal region that mediates covalent cross-linking to the wall matrix through modified glycosylphosphatidylinositol (GPI) anchors.[10] Tandem repeats in Als proteins form a string of compact subdomains that have nonspecific hydrophobic interactions with a variety of fungal and host protein structures, and can be unfolded by mechanical force.[11,12] Whether such hydrophobic forces are also found in Epa proteins is not known.

Hydrophobic interactions are of great relevance in microbial pathogenesis as they contribute to promote the adhesion of pathogens to abiotic surfaces and tissues.[13] Hydrophobic forces are recognized as being an important driving force for fungal adhesion,[14−16] but their molecular origin is poorly understood. Although various approaches are available for probing microbial cell surface hydrophobicity, the direct measurement of hydrophobic forces on microorganisms has been a longstanding challenge. During the past years, atomic force microscopy (AFM) has offered new opportunities to address this issue.[17,18] On the one hand, chemical force microscopy (CFM) with hydrophobic tips has proved to be a powerful tool for probing local hydrophobic forces on microbial cell surfaces.[19−23] On the other hand, single-cell force spectroscopy (SCFS) allows researchers to quantify the interaction forces between single whole cells and hydrophobic substrates.[24−27] Here, we combine the two modalities to decipher the role of hydrophobic forces in the adhesion of *C. glabrata*, focusing on the Epa6 adhesin. The results provide the first direct piece of evidence that Epa6 is engaged in strong hydrophobic interactions with abiotic surfaces, which we expect to be critical to biofilm formation and associated infections.

RESULTS AND DISCUSSION

Epa6 Is Involved in Yeast Adhesion and Biofilm Formation. We first studied the involvement of Epa6 in cell adhesion and biofilm formation at the microscopic level (Figure 1). The ability of *C. glabrata* to form biofilms represents an important medical aspect of this fungus. Despite the lack of yeast-to-hyphae transition, a crucial phenomenon for *C. albicans* biofilm development, *C. glabrata* is known to form multilayer biofilm structures composed of only yeast cells. Cells from *C. glabrata* wild type strain (WT) and *C. glabrata epa6* deletion strain (*epa6*Δ) were let to attach to 96-well polystyrene plates, which represent a favorable substrate for *Candida* biofilm formation. Adhering and biofilm-forming cells were assessed by the XTT reduction assay measured at 490 nm. Figure 1a shows the average XTT measured metabolic activities for adhering and biofilm-associated cells. There were striking differences (statistically significant, $p \leq 0.0001$) both in adhesion and biofilm formation between WT and *epa6*Δ cells, thus indicating that Epa6 is involved in yeast adhesion and in the formation of biofilms. These differences were further supported by direct live-cell imaging using confocal microscopy, as shown in Figure 1b,c. While WT cells exhibited multilayer biofilm structures spread over the whole plastic surface, *epa6*Δ cells exhibited only small amounts of attached cells.

Single-Cell Force Spectroscopy Reveals That Epa6 Mediates Strongly Adhesive Interactions between Yeast Cells and Hydrophobic Surfaces. In light of the above microscopic data, we postulated that Epa6-mediated adhesion is primarily governed by hydrophobic forces. To test this hypothesis, we quantified the interaction forces between single *C. glabrata* cells and solid substrates using a noninvasive SCFS assay (Figure 2).[24,25,28,29] Tipless cantilevers were coated with polydopamine, slowly approached toward single cells deposited on a glass Petri dish in buffer, kept in contact for 1 min, and then withdrawed. Force−distance curves were measured

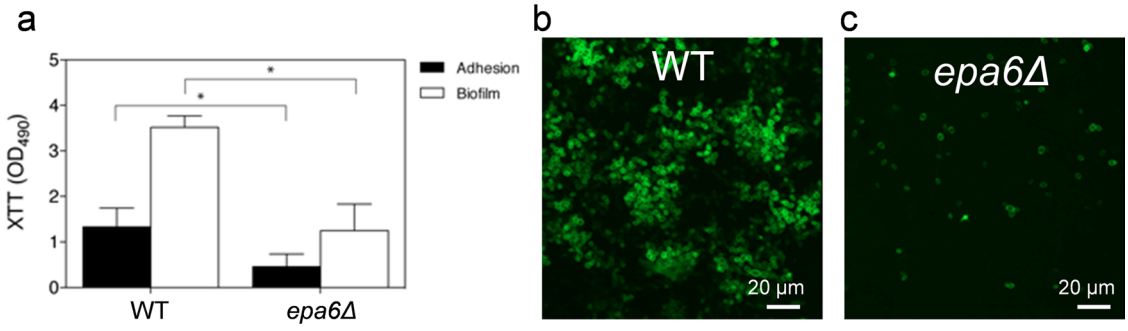

Figure 1. *C. glabrata* cells lacking Epa6 adhesins (*epa6*Δ mutant) fail to adhere and to form mature biofilms on polystyrene. (a) Ability of *C. glabrata* WT and *C. glabrata epa6*Δ to adhere and to form mature biofilms in 96-well polystyrene plates in RPMI 1640 medium at 37 °C. Standard deviations were calculated from three independent experiments and statistical significance was documented when *$p \leq 0.0001$. (b and c) Confocal scanning laser microscopy images of mature (24 h old) biofilms stained with Concanavalin A, Alexa Fluor 488 conjugate (50 mg L^{-1}, green fluorescence) at 37 °C for 1 h. *C. glabrata* WT formed multilayer structures (b), whereas *C. glabrata epa6*Δ exhibited only scattered amount of yeast cells on the surface (c).

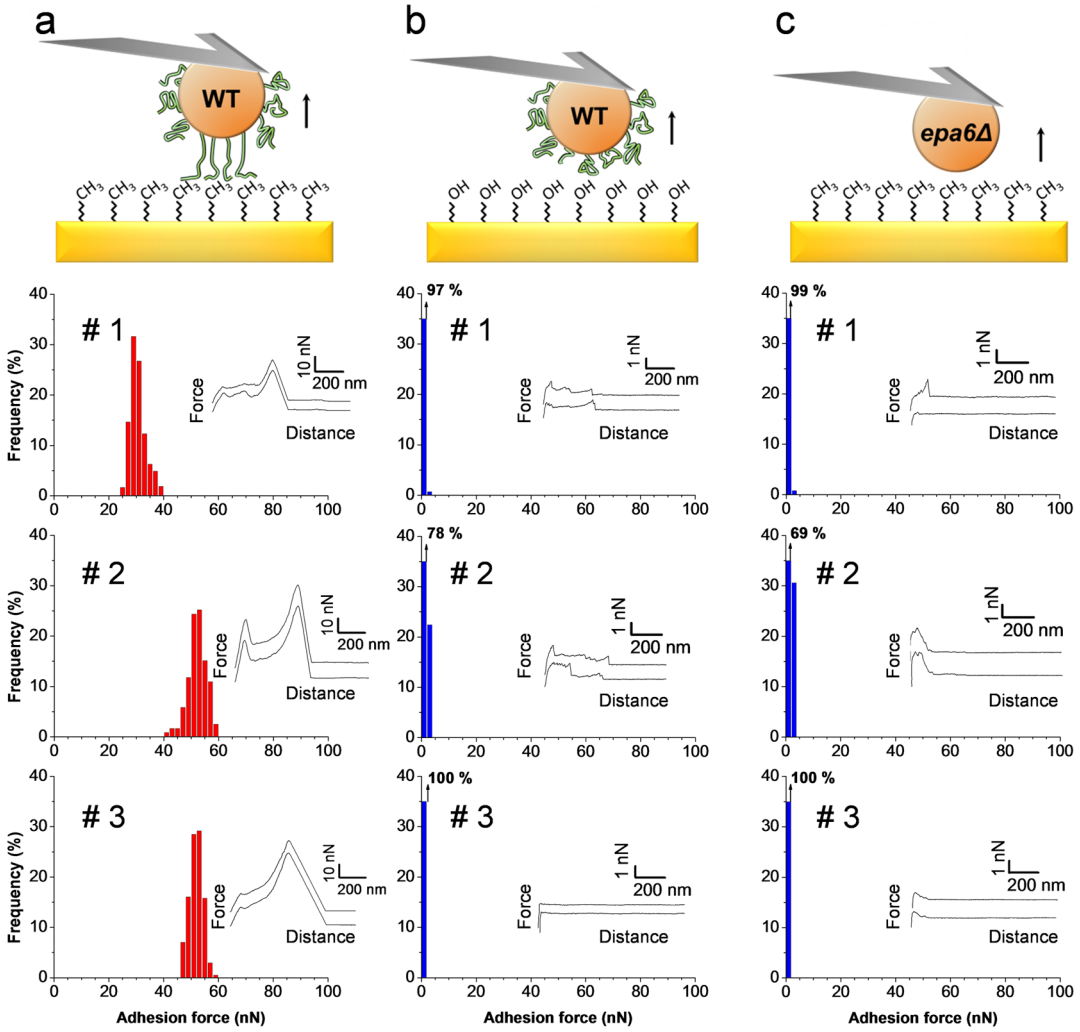

Figure 2. Single-cell force spectroscopy unravels Epa6-mediated hydrophobic interactions. (a and b) Adhesion force histograms and representative retraction force profiles obtained in acetate buffer by recording multiple force−distance curves between three different WT cells and (a) hydrophobic substrates (n = 430, 119, and 411 curves for cells 1, 2 and 3) or (b) hydrophilic substrates (n = 425, 451, and 104 curves). (c) Force data obtained for the interaction between the *epa6*Δ mutant strain impaired in Epa6 expression and hydrophobic substrates (n = 108, 109, and 137 curves). All curves were obtained using a contact time of 100 ms, a maximum applied force of 500 pN, and approach and retraction speeds of 1.0 μm s^{-1}. For more cells, see Table 1.

between single-cell probes and hydrophobic (methyl-terminated) or hydrophilic (hydroxyl-terminated) substrates. Figure 2a shows the maximum adhesion forces and representative force curves obtained between 3 different WT cells and hydrophobic substrates (for more cells, see Table 1). The adhesion probability was always 100% and all the curves showed large adhesion forces (cell #1, 30.6 ± 3 nN, mean ± SD on n = 430 force curves; cell #2, 52.2 ± 3 nN, n = 119; cell #3, 51.8 ± 2 nN, n = 411). Recording multiple force curves with the same single cell did not alter the general shape of the curves. Although different cells generally showed similar adhesion force profiles, there were some variations from one cell to another (Table 1), suggesting that the cell population was heterogeneous. Interestingly, the strong adhesion force, also named maximum detachment force, showed large extension (500−1500 nm)

TABLE 1. Probability of Adhesion (P_{adh} = % of Curves with Adhesion Force >2 nN) and Mean Adhesion Force (F_{adh}) Measured by Single-Cell Force Spectroscopy on 10 Different WT and *epa6*Δ Cells

WT *vs* CH_3		WT *vs* OH		*epa6*Δ *vs* CH_3	
P_{adh} (%)	F_{adh} (nN)	P_{adh} (%)	F_{adh} (nN)	P_{adh} (%)	F_{adh} (nN)
100	30.6 ± 3	3	0.9 ± 0.3	1	0.6 ± 0.4
100	52.2 ± 3	22	1.8 ± 0.3	31	1.9 ± 0.5
100	51.8 ± 2	0	0.1 ± 0.1	0	1.3 ± 0.1
100	31.7 ± 1	1	1.1 ± 0.4	0	0.7 ± 0.1
100	46.1 ± 9	0	0.4 ± 0.3	0	0.7 ± 0.1
100	31.1 ± 3	0	1.1 ± 0.4	97	4.8 ± 1.4
100	34.6 ± 6	0	0.8 ± 0.1	0	0.2 ± 0.1
100	33.5 ± 4	0	0.1 ± 0.3	49	2.5 ± 1.8
100	16.9 ± 1	0	0.7 ± 0.3	81	2.5 ± 0.5
100	23.7 ± 3	0	1.8 ± 0.1	84	2.7 ± 0.8

and was generally preceded by multiple smaller adhesion events, documenting protein unfolding. As the average force (up to ~50 nN) is up to 200 times larger than that associated with the adhesion force of single fungal adhesins (~250 pN, see below),[11,12] we hypothesize that these signatures correspond to the unfolding of at least ~200 adhesins. Finally, the detachment force always showed a sharp rupture, suggesting multiple proteins were stretched and detached simultaneously from the substrate, possibly as large clusters.

To gain further insight into the origin of the measured forces, two additional experiments were carried out. First, we measured the adhesion forces toward hydrophilic, hydroxyl-terminated surfaces. Figure 2b and Table 1 show that adhesion forces were much less frequent and much weaker, indicating that the large adhesion forces are mostly hydrophobic in nature. Long extensions similar to those seen on hydrophobic surfaces were observed, suggesting that the weaker forces were also associated with protein unfolding. Second, the *epa6*Δ mutant strain impaired in Epa6 expression (Figure 2c and Table 1) exhibited adhesion forces that were again much smaller, less frequent and with much shorter extensions, compared to WT cells. These observations lead us to believe that hydrophobic interactions of single *C. glabrata* cells are primarily mediated by Epa6 proteins, and that these interactions involve binding and unfolding of multiple Epa6 molecules.

Chemical Force Microscopy Shows That Epa6 Is Massively Exposed on Yeast Cells and Conveys Strong Hydrophobic Properties to Their Surface. To provide a direct demonstration that Epa6 contributes to cell surface hydrophobicity, we probed *C. glabrata* cells with nanoscale resolution using tips functionalized with hydrophobic groups (CH_3) (Figure 3). Topographic imaging revealed a

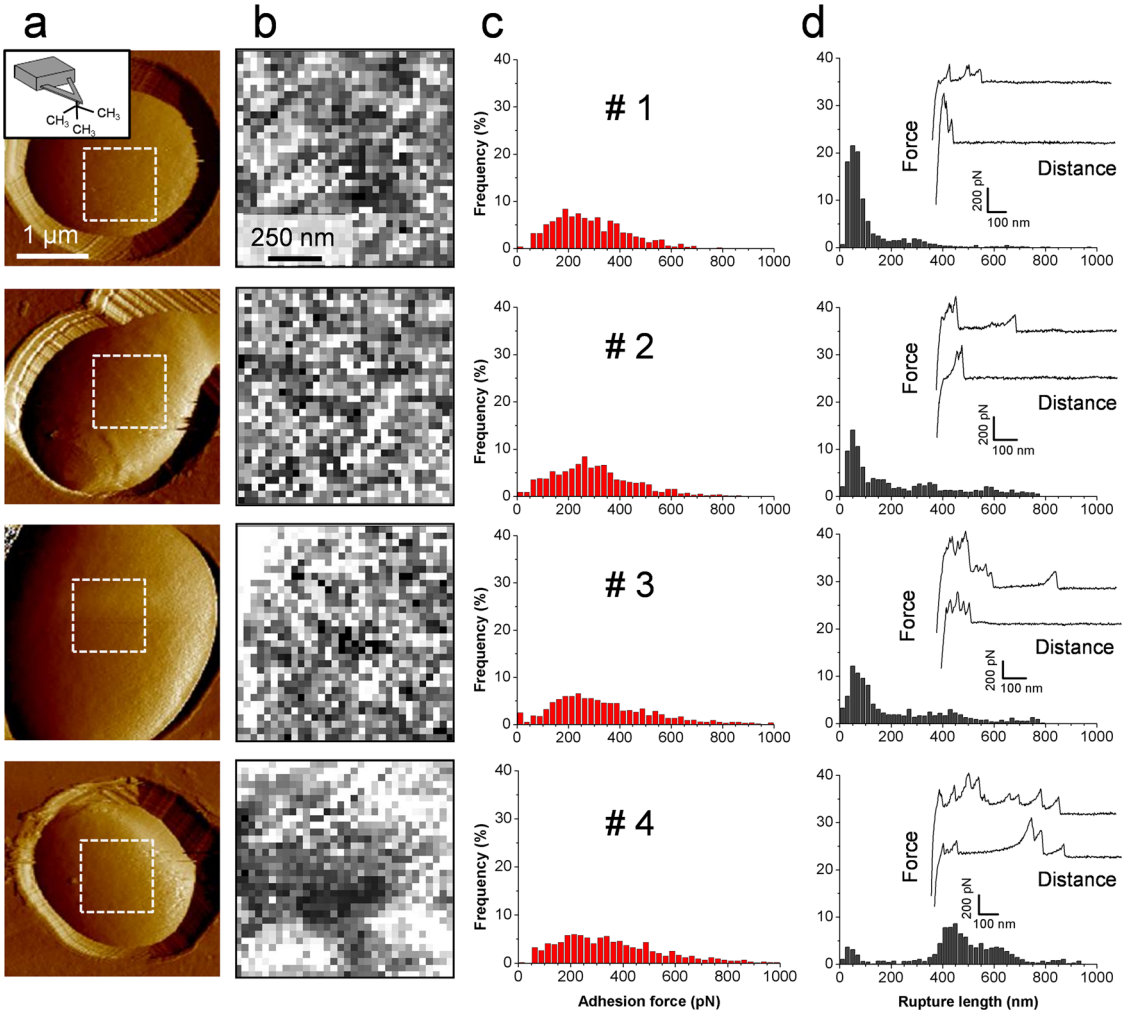

Figure 3. Mapping and quantifying hydrophobic forces on *C. glabrata* cells using chemical force microscopy. (a) AFM deflection images of 4 different *C. glabrata* WT cells recorded in acetate buffer with silicon nitride tips. The white squares indicate the regions where the force maps were recorded. (b) Adhesion force maps (1 μm × 1 μm; *z* range = 500 pN; bright pixels correspond to hydrophobic binding events), (c) adhesion force histograms, and (d) rupture length histograms with representative force curves obtained by recording spatially resolved force curves on the cell surfaces using hydrophobic tips (*n* = 1024 curves for each cell). All curves were obtained using a contact time of 100 ms, a maximum applied force of 500 pN, and approach and retraction speeds of 1.0 μm s^{-1}. Similar results were obtained in a total of 10 different cells.

smooth cell surface, consistent with earlier electron microscopy and AFM studies.[8,30,31] Most force curves recorded on WT cells featured adhesion forces of 258 ± 153 pN magnitude (mean ± SD from 10 240 curves obtained on 10 different cells). A substantial fraction of these curves (from 5%, cell #1, to 90%, cell #4) showed multiple adhesion peaks, together with extended rupture lengths (200−800 nm). Hence, while there were variations from one cell to another, reflecting heterogeneity of the cell population, adhesive curves generally showed common features, *i.e.*, adhesion forces of about 250 pN and multiple adhesion events with long extensions. We believe that these features reflect essentially the unfolding of Epa6 proteins as they were markedly altered in the *epa6*Δ mutant, *i.e.*, most curves featured smaller adhesion forces, 160 ± 103 pN magnitude (mean ± SD from 8192 curves obtained on 8 different cells), and shorter ruptures than those on WT cells (Figure 4). Do the rupture lengths on WT cells correspond to the lengths of fully extended Epa proteins? Epa proteins are about 700 amino acids in length.[7,32,33] Therefore, assuming that each amino acid contributes 0.36 nm to the contour length of a fully extended polypeptide chain, the length of a fully extended adhesin is expected to be 250 nm. While some rupture lengths were close to this value, much longer extensions were also observed depending on the cell investigated. In SCFS experiments, even larger extensions were observed (500−1500 nm). Given the very high surface concentration of Epa proteins (see below), we suggest that some Epa proteins are bound together in aggregates and one is released from its own GPI but still anchored to another protein until a certain length is reached. Alternatively, deletion of Epa6 may change the expression of other Epa genes or other cell wall protein

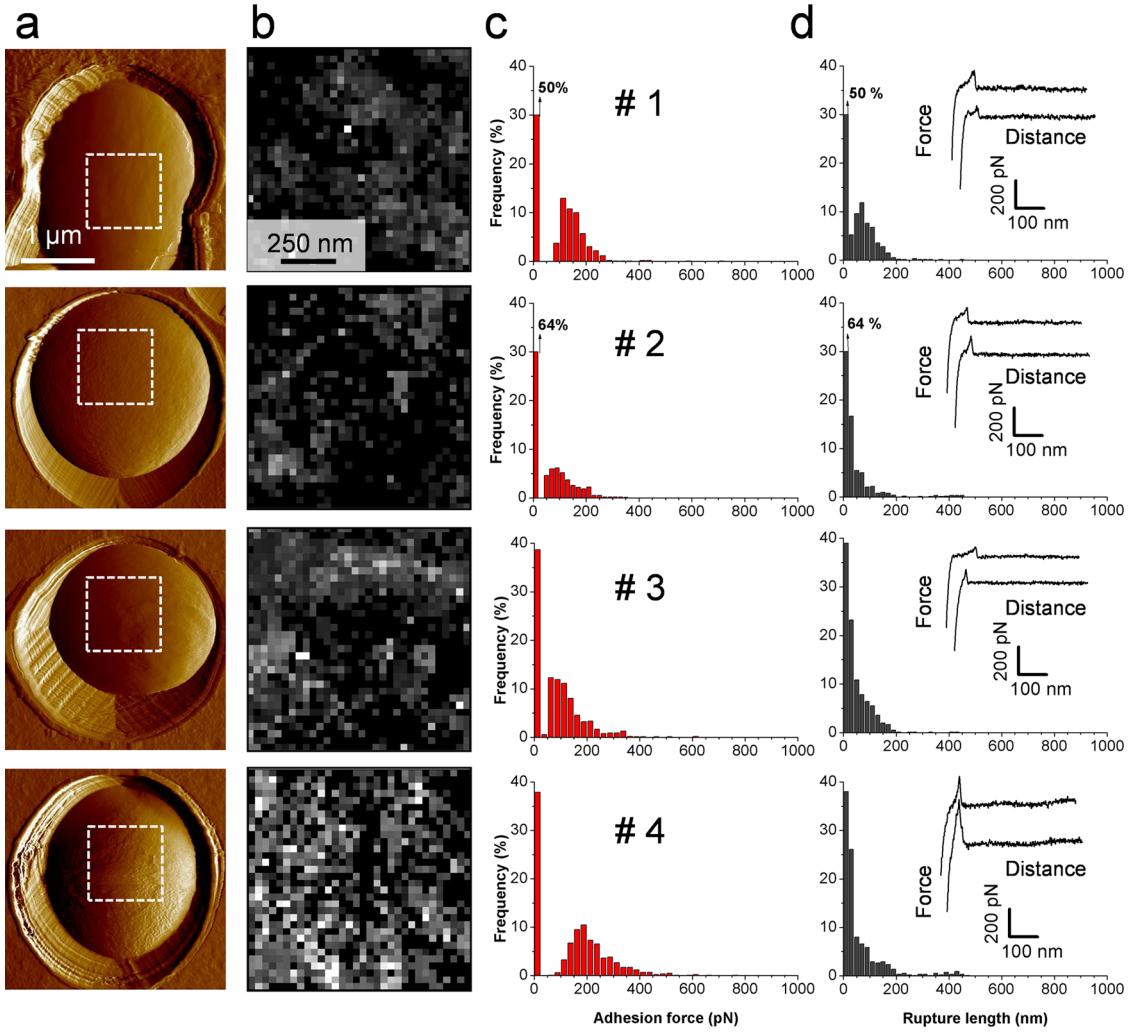

Figure 4. Chemical force microscopy reveals much weaker hydrophobic forces on *epa6*Δ mutant cells. (a) AFM deflection images of 4 different *C. glabrata epa6*Δ cells recorded in acetate buffer with silicon tips. (b) Adhesion force maps (1 μm × 1 μm; *z* range = 500 pN), (c) adhesion force histograms, and (d) rupture length histograms with representative force curves obtained by recording spatially resolved force curves on the cell surfaces using hydrophobic tips (*n* = 1024 curves for each cell). All curves were obtained using a contact time of 100 ms, a maximum applied force of 500 pN, and approach and retraction speeds of 1.0 μm s^{-1}. Similar results were obtained in a total of 8 different cells.

encoding genes. The average unfolding force, ~250 pN, is in the range of the force needed to unravel proteins rich in β-sheet structures.[34] A striking observation was that sawtooth patterns were generally lacking in the Epa6 force profiles, which is in contrast with the mechanical behavior of Als adhesins.[11,12] This could reflect structural differences in the adhesins: while Als and Flo proteins contain large amounts of tandem repeats that are sequentially unravelled by force, Epa6 would contain few (no) repeats in the strain that we used.[35] Accordingly, our CFM experiments indicate that cell surface hydrophobicity in *C. glabrata* originates from Epa6 proteins, and that the associated hydrophobic forces involve, to some extent, unfolding of the adhesins. As Epa6 is rich in hydrophobic residues (35%), it is tempting to speculate that, upon mechanical stress, Epa6 proteins will unfold and expose hydrophobic residues, thereby promoting further hydrophobic interactions with solid substrates (here, the AFM tip).

Finally, adhesion maps showed a very high detection level that correspond to a minimum protein surface density of ~1000 sites/μm^2 (assuming each binding event corresponds to a single protein), indicating that the adhesins were massively exposed. Note that given our large pixel size (30 nm) and the very high surface concentration of adhesins, it is likely that the actual protein density is larger. These CFM-based values may be compared with the protein density estimated from our SCFS adhesion force values, suggesting that up to ~200 adhesins are probed, and considering the cell–substrate contact area.[24] As a rough approximation, the contact zone of a deformable sphere pressed on a rigid flat surface may be estimated by $A = \pi R\delta$, in which A is the contact area, R is the radius of the cell, and δ is the cell deformation. Considering a cell radius of 2 μm and a deformation of ~10 nm (estimated from indentation curves), we found a contact area of ~0.06 μm^2, thus yielding a protein surface density of ~3300 proteins/μm^2. Considering the size and flexibility of Epa proteins, the actual interacting area is probably larger than 0.06 μm^2, meaning this density would be overestimated. Also, we note (i) that some adhesion events in our CFM measurements may reflect the detection of multiple proteins, rather than single proteins, and (ii) that SCFS and CFM adhesion forces showed substantial variations from one cell to another. These factors will increase the error on the calculation, which should therefore be considered as a rough estimate. Taking this into consideration, the 3300 proteins/μm^2 value is larger than the 1000 proteins/μm^2 minimum density that we measured by CFM, suggesting that this method underestimates the actual amount of cell surface proteins. We expect that the very high cell surface concentration of adhesins will increase the strength and duration of cellular adhesion, as observed in SCFS experiments.

CONCLUSIONS

Biofilm formation is known to be critical to fungal pathogenesis, but the underlying molecular mechanisms are not fully understood. We have shown that SCFS and CFM are two powerful AFM-based techniques for probing hydrophobic forces on fungal pathogens, and for understanding their role in cell adhesion. We found that (i) single *C. glabrata* cells strongly bind to hydrophobic substrates using their surface-associated Epa6 proteins, (ii) Epa6 adhesins are widely expressed at the yeast cell surface, and (iii) they are engaged in strong hydrophobic interactions with abiotic surfaces. We suggest that during cell–substrate contact, mechanical stress may enhance the exposure of Epa6 hydrophobic sequences that will strengthen adhesion.

METHODS

Strains and Growth Conditions. *C. glabrata* ATCC2001 (American Type Culture Collection CBS138) and *C. glabrata epa6*Δ[8] (kindly provided by G. Janbon, Institut Pasteur, France) were grown routinely on YPD (1% yeast extract, 2% peptone, 2% glucose) agar plates at 37 °C. Before all experiments, both strains were incubated in liquid YPD medium for at least 24 h at 37 °C (stationary phase).

Adhesion and Biofilm Development. For *in vitro C. glabrata* biofilm tests, cells were collected from YPD cultures and washed twice with PBS. RPMI 1640 medium (with L-glutamine and phenol red) without bicarbonate was buffered with 3-(*N*-morpholino)-propanesulfonic acid (Sigma). The pH of the medium was adjusted to 7.0 with 1 M NaOH. Biofilm development was studied in 96-well polystyrene plates. Briefly, *C. glabrata* cells at a final concentration of 1×10^6 cells mL^{-1} were allowed to attach onto the polystyrene substrate during the period of adhesion (90 min, 37 °C, static). Then, nonadhering cells were removed by washing with PBS, and cells associated with the substrate were subsequently submerged in fresh RPMI 1640 medium for 24 h (mature biofilm development). Adhering and biofilm-forming cells were evaluated for their metabolic activity by the reduction of the substrate XTT [2,3-bis(2-methoxy-4-nitro-5-sulfophenyl)-2*H*-tetrazolium-5-carboxanilide] to XTT formazan by mitochondrial dehydrogenases of metabolic active cells (Ramage *et al.*[36]). The XTT working solution was prepared in sterile PBS at a final concentration 1 mg/mL. Before use, menadione was added to the XTT solution (final concentration 1 μM). This solution was vortexed and 100 μL was applied into each well containing adhered or biofilm-forming cells. Plates were incubated for 1 h at 37 °C in the dark. The intensity of colorimetric change was measured with a spectrophotometer (Spectra max Plus 384) at 490 nm. The XTT-menadione solution without *Candida* cells was used as a blank. Statistical analyses were performed using Student's *t*-test (GraphPad Prism software). Differences were considered significant if $*p \leq 0.0001$. All *in vitro C. glabrata* adhesion and biofilm experiments performed in 96-well polystyrene plates were repeated three times always using 6 wells per strain.

Confocal Scanning Laser Microscopy. For confocal microscopy, *C. glabrata* biofilms were formed on plastic highly adhesive round tissue culture coverslips (13 mm diameter, Sarstedt, Germany). One milliliter of *C. glabrata* suspension prepared in RPMI 1640 medium was added to wells containing coverslips

(one per well) and the samples were incubated for 90 min at 37 °C. The coverslips were gently washed twice with PBS, placed in a clean 24-well tissue culture plate and covered with fresh medium for additional 24 h. Mature biofilms were washed with PBS and subsequently stained with Concanavalin A (ConA, 50 mg L^{-1}), Alexa Fluor 488 conjugate (Molecular Probes, Eugene, OR) at 37 °C for 1 h (green fluorescence). Imaging was carried out with an Olympus FV1000 confocal laser scanning biological microscope and images were processed with the accompanying software, FV10-ASW 2.0.

Chemical Force Microscopy. Hydrophobic, methyl-terminated AFM tips were prepared by immersing gold-coated cantilevers (OMCL-TR4, Olympus Ltd., Tokyo, Japan; nominal spring constant ~0.02 N m^{-1}) for 12 h in 1 mM solutions of 1-dodecanethiol (Sigma-Aldrich, 98%) in ethanol and then rinsed with ethanol and dried with N_2. CFM measurements were performed at room temperature (20 °C) in sodium acetate buffer, using a Nanoscope VIII Multimode AFM from Bruker Corporation (Santa Barbara, CA). The spring constants of the cantilevers were measured using the thermal noise method. Yeast cells were immobilized by mechanical trapping into porous polycarbonate membranes (Millipore, Billerica, MA) with a pore size similar to the cell size.[37,38] After filtering a cell suspension, the filter was gently rinsed with buffer, carefully cut (1 cm × 1 cm), attached to a steel sample puck using a small piece of double face adhesive tape, and the mounted sample was transferred into the AFM liquid cell while avoiding dewetting. Single yeast cells were first localized using a bare tip, after which the tip was replaced with a methyl-terminated tip for force measurements (see ref 38 for details). We recorded force maps of 32 × 32 force−distance curves on areas of 1 μm^2 with a maximum applied force of 500 pN, a contact time of 100 ms, and an approach and retract tip velocity of 1000 nm s^{-1}. Adhesion maps were obtained by calculating the largest adhesion force for each force curve and displaying the value as a gray pixel. Adhesion and rupture length histograms were obtained by considering, in each curve, the largest adhesion forces and last rupture distances, respectively.

Single-Cell Force Spectroscopy. For SCFS, hydrophobic and hydrophilic substrates were prepared by immersing gold-coated substrates in ethanol solutions containing 1 mM 1-dodecanethiol (Sigma-Aldrich, 98%) or 1 mM 11-mercapto- 1-undecanol (Sigma-Aldrich, 97%) overnight, rinsing them with ethanol and drying them under N_2. For cell probe preparation,[29] tipless Si_3N_4 cantilevers with a nominal spring constant of ~0.12 N m^{-1} (NP-O10 levers, Bruker) were immersed for 1 h in 10 mM Tris buffer solution (pH 8.5) containing 4 mg mL^{-1} dopamine hydrochloride. The cantilever was then washed and dried under N_2. The dopamine coated cantilever was brought into contact with an isolated cell deposited in the bottom of a glass Petri dish for 1 min, and the obtained cell probe was transferred over hydrophilic or hydrophobic substrates without dewetting. The spring constants of the cantilevers were measured using the thermal noise method. SCFS measurements were performed at room temperature (20 °C) in sodium acetate buffer, using a Bioscope Catalyst AFM (Bruker Corporation, Santa Barbara, CA). A minimum of 100 force−distance curves for each cell were recorded on three different spots on a given substrate with a maximum applied force of 500 pN, a contact time of 100 ms, and constant approach and retract speeds of 1000 nm s^{-1}. Adhesion force histograms were obtained by calculating the maximum adhesion force.

Conflict of Interest: The authors declare no competing financial interest.

Acknowledgment. Work at the Université Catholique de Louvain was supported by the National Fund for Scientific Research (FNRS), the Université Catholique de Louvain (Fonds Spéciaux de Recherche), the Federal Office for Scientific, Technical and Cultural Affairs (Interuniversity Poles of Attraction Programme), and the Research Department of the Communauté française de Belgique (Concerted Research Action). Work in the lab of P.V.D. was supported by the Fund for Scientific Research Flanders (FWO project VS.036.14N). Y.F.D. is a Research Director at the FNRS. SK was supported by postdoctoral grants of the KU Leuven (PDMK 11/089) and FWO.

REFERENCES AND NOTES

1. Douglas, L. J. *Candida* Biofilms and Their Role in Infection. *Trends Microbiol.* **2003**, *11*, 30–36.
2. Finkel, J. S.; Mitchell, A. P. Genetic Control of *Candida albicans* Biofilm Development. *Nat. Rev. Microbiol.* **2011**, *9*, 109–118.
3. Verstrepen, K. J.; Klis, F. M. Flocculation, Adhesion and Biofilm Formation in Yeasts. *Mol. Microbiol.* **2006**, *60*, 5–15.
4. Fanning, S.; Mitchell, A. P. Fungal Biofilms. *PLoS Pathog.* **2012**, *8*, e1002585.
5. Kaur, R.; Domergue, R.; Zupancic, M. L.; Cormack, B. P. A Yeast by Any Other Name: *Candida glabrata* and Its Interaction with the Host. *Curr. Opin. Microbiol.* **2005**, *8*, 378–384.
6. Roetzer, A.; Gabaldon, T.; Schuller, C. From *Saccharomyces cerevisiae* to *Candida glabrata* in a Few Easy Steps: Important Adaptations for an Opportunistic Pathogen. *FEMS Microbiol. Lett.* **2011**, *314*, 1–9.
7. Cormack, B. P.; Ghori, N.; Falkow, S. An Adhesin of the Yeast Pathogen *Candida glabrata* Mediating Adherence to Human Epithelial Cells. *Science* **1999**, *285*, 578–582.
8. Iraqui, I.; Garcia-Sanchez, S.; Aubert, S.; Dromer, F.; Ghigo, J. M.; d'Enfert, C.; Janbon, G. The Yak1p Kinase Controls Expression of Adhesins and Biofilm Formation in *Candida glabrata* in a Sir4p-Dependent Pathway. *Mol. Microbiol.* **2005**, *55*, 1259–1271.
9. Riera, M.; Mogensen, E.; d'Enfert, C.; Janbon, G. New Regulators of Biofilm Development in *Candida glabrata*. *Res. Microbiol.* **2012**, *163*, 297–307.
10. Dranginis, A. M.; Rauceo, J. M.; Coronado, J. E.; Lipke, P. N. A Biochemical Guide to Yeast Adhesins: Glycoproteins for Social and Antisocial Occasions. *Microbiol. Mol. Biol. Rev.* **2007**, *71*, 282–294.
11. Alsteens, D.; Dupres, V.; Klotz, S. A.; Gaur, N. K.; Lipke, P. N.; Dufrêne, Y. F. Unfolding Individual Als5p Adhesion Proteins on Live Cells. *ACS Nano* **2009**, *3*, 1677–1682.
12. Alsteens, D.; Garcia, M. C.; Lipke, P. N.; Dufrêne, Y. F. Force-Induced Formation and Propagation of Adhesion Nanodomains in Living Fungal Cells. *Proc. Natl. Acad. Sci. U.S.A.* **2010**, *107*, 20744–20749.
13. Doyle, R. J. Contribution of the Hydrophobic Effect to Microbial Infection. *Microbes Infect.* **2000**, *2*, 391–400.
14. Ener, B.; Douglas, L. J. Correlation Between Cell-Surface Hydrophobicity of *Candida albicans* and Adhesion to Buccal Epithelial Cells. *FEMS Microbiol. Lett.* **1992**, *78*, 37–42.
15. Masuoka, J.; Hazen, K. C. Cell Wall Protein Mannosylation Determines *Candida albicans* Cell Surface Hydrophobicity. *Microbiology* **1997**, *143*, 3015–3021.
16. Yoshijima, Y.; Murakami, K.; Kayama, S.; Liu, D.; Hirota, K.; Ichikawa, T.; Miyake, Y. Effect of Substrate Surface Hydrophobicity on the Adherence of Yeast and Hyphal *Candida*. *Mycoses* **2010**, *53*, 221–226.
17. Alsteens, D.; Beaussart, A.; El-Kirat-Chatel, S.; Sullan, R. M.; Dufrêne, Y. F. Atomic Force Microscopy: A New Look at Pathogens. *PLoS Pathog.* **2013**, *9*, e1003516.
18. Dufrêne, Y. F. Atomic Force Microscopy in Microbiology: New Structural and Functional Insights into the Microbial Cell Surface. *mBio* **2014**, *5*, e01363–14.
19. Alsteens, D.; Dague, E.; Rouxhet, P. G.; Baulard, A. R.; Dufrêne, Y. F. Direct Measurement of Hydrophobic Forces on Cell Surfaces Using AFM. *Langmuir* **2007**, *23*, 11977–11979.
20. Dague, E.; Alsteens, D.; Latge, J. P.; Verbelen, C.; Raze, D.; Baulard, A. R.; Dufrêne, Y. F. Chemical Force Microscopy of Single Live Cells. *Nano Lett.* **2007**, *7*, 3026–3030.
21. Dague, E.; Alsteens, D.; Latge, J. P.; Dufrêne, Y. F. High-Resolution Cell Surface Dynamics of Germinating *Aspergillus fumigatus* Conidia. *Biophys. J.* **2008**, *94*, 656–660.
22. Beaussart, A.; Alsteens, D.; El-Kirat-Chatel, S.; Lipke, P. N.; Kucharíková, S.; Van Dijck, P.; Dufrêne, Y. F. Single-Molecule Imaging and Functional Analysis of Als Adhesins and Mannans during *Candida albicans* Morphogenesis. *ACS Nano* **2012**, *6*, 10950–10964.

23. El-Kirat-Chatel, S.; Beaussart, A.; Alsteens, D.; Jackson, D. N.; Lipke, P. N.; Dufrêne, Y. F. Nanoscale Analysis of Caspofungin-Induced Cell Surface Remodelling in *Candida albicans*. *Nanoscale* **2013**, *5*, 1105–1115.
24. Alsteens, D.; Beaussart, A.; Derclaye, S.; El-Kirat-Chatel, S.; Park, H. R.; Lipke, P. N.; Dufrêne, Y. F. Single-Cell Force Spectroscopy of Als-Mediated Fungal Adhesion. *Anal. Methods* **2013**, *5*, 3657–3662.
25. Beaussart, A.; El-Kirat-Chatel, S.; Herman, P.; Alsteens, D.; Mahillon, J.; Hols, P.; Dufrêne, Y. F. Single-Cell Force Spectroscopy of Probiotic Bacteria. *Biophys. J.* **2013**, *104*, 1886–1892.
26. Tripathi, P.; Beaussart, A.; Alsteens, D.; Dupres, V.; Claes, I.; von Ossowski, I.; de Vos, W. M.; Palva, A.; Lebeer, S.; Vanderleyden, J.; *et al.* Adhesion and Nanomechanics of Pili From the Probiotic *Lactobacillus rhamnosus* GG. *ACS Nano* **2013**, *7*, 3685–3697.
27. El-Kirat-Chatel, S.; Beaussart, A.; Boyd, C. D.; O'Toole, G. A.; Dufrêne, Y. F. Single-Cell and Single-Molecule Analysis Deciphers the Localization, Adhesion, and Mechanics of the Biofilm Adhesin LapA. *ACS Chem. Biol.* **2014**, *9*, 485–494.
28. Alsteens, D.; Van Dijck, P.; Lipke, P. N.; Dufrêne, Y. F. Quantifying the Forces Driving Cell-Cell Adhesion in a Fungal Pathogen. *Langmuir* **2013**, *29*, 13473–13480.
29. Beaussart, A.; El-Kirat-Chatel, S.; Sullan, R. M.; Alsteens, D.; Herman, P.; Derclaye, S.; Dufrêne, Y. F. Quantifying the Forces Guiding Microbial Cell Adhesion using Single-Cell Force Spectroscopy. *Nat. Protoc.* **2014**, *9*, 1049–1055.
30. de Groot, P. W.; Kraneveld, E. A.; Yin, Q. Y.; Dekker, H. L.; Gross, U.; Crielaard, W.; de Koster, C. G.; Bader, O.; Klis, F. M.; Weig, M. The Cell Wall of the Human Pathogen *Candida glabrata*: Differential Incorporation of Novel Adhesin-like Wall Proteins. *Eukaryotic Cell* **2008**, *7*, 1951–1964.
31. El-Kirat-Chatel, S.; Beaussart, A.; Alsteens, D.; Sarazin, A.; Jouault, T.; Dufrêne, Y. F. Single-Molecule Analysis of the Major Glycopolymers of Pathogenic and Non-Pathogenic Yeast Cells. *Nanoscale* **2013**, *5*, 4855–4863.
32. Castano, I.; Pan, S. J.; Zupancic, M.; Hennequin, C.; Dujon, B.; Cormack, B. P. Telomere Length Control and Transcriptional Regulation of Subtelomeric Adhesins in *Candida glabrata*. *Mol. Microbiol.* **2005**, *55*, 1246–1258.
33. De Las Penas, A.; Pan, S. J.; Castano, I.; Alder, J.; Cregg, R.; Cormack, B. P. Virulence-Related Surface Glycoproteins in the Yeast Pathogen *Candida glabrata* Are Encoded in Subtelomeric Clusters and Subject to Rap1- and Sir-Dependent Transcriptional Silencing. *Genes Dev.* **2003**, *17*, 2245–2258.
34. Rief, M.; Gautel, M.; Oesterhelt, F.; Fernandez, J. M.; Gaub, H. E. Reversible Unfolding of Individual Titin Immunoglobulin Domains by AFM. *Science* **1997**, *276*, 1109–1112.
35. Thierry, A.; Bouchier, C.; Dujon, B.; Richard, G. F. Megasatellites: A Peculiar Class of Giant Minisatellites in Genes Involved in Cell Adhesion and Pathogenicity in *Candida glabrata*. *Nucleic Acids Res.* **2008**, *36*, 5970–5982.
36. Ramage, G.; Vandewalle, K.; Wickes, B. L.; Lopez-Ribot, J. L. Characteristics of Biofilm Formation by *Candida albicans*. *Rev. Iberoam. Micol.* **2001**, *18*, 163–170.
37. Kasas, S.; Ikai, A. A Method for Anchoring Round Shaped Cells for Atomic Force Microscope Imaging. *Biophys. J.* **1995**, *68*, 1678–1680.
38. Dufrêne, Y. F. Atomic Force Microscopy and Chemical Force Microscopy of Microbial Cells. *Nat. Protoc.* **2008**, *3*, 1132–1138.